Joint Pathology Center
Veterinary Pathology Services

WEDNESDAY SLIDE CONFERENCE 2019-2020

# C o n f e r e n c e 19   19 February 2020

Conference Moderator:

Molly Church, VMD, Ph.D, DACVP
Assistant Professor, Pathobiology
University of Pennsylvania School of Veterinary Medicine
4005 MJR-VHUP
3900 Delancey Street
Philadelphia, PA, 19104

CASE I: 17041318 (JPC 4117490).

Signalment: 3-month-old, female, Aberdeen-Angus calf (*Bos taurus*)

History: Paraparesis and inability to stand with the hindlimbs were noted for 6 days. Clinical signs were not improved with penicillin treatments and progressed to lateral recumbency and hindlimb paralysis. Rigidity of the head and neck was noted. The calf had no deep pain and no patellar reflex in both hindlimbs, whereas deep pain was normal in the forelimbs. Cranial nerve responses were intact and normal. Omphalitis was present, and body temperature, pulse and respiratory rates were normal. The calf was euthanized and submitted for necropsy.

Gross Pathology: Multiple pale white streaks were seen on the epicardium. On cut surfaces of the heart, multiple irregular, pale white foci were observed in the myocardium, especially in the papillary muscle. Similar pale white streaks and irregular pale foci were noted in the skeletal muscles throughout the body, including the shoulders, brisket, quadriceps, and tongue.
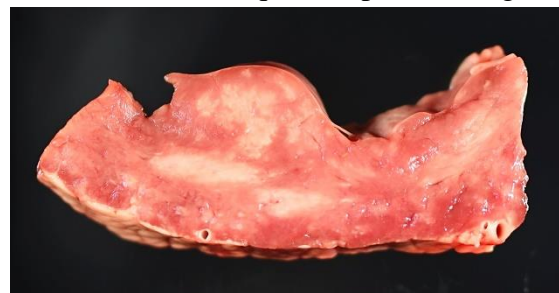
Heart, calf. The cut surface of the myocardium demonstrates numerous irregular pale white foci. (Photo courtesy of: Oklahoma State University, Department of Veterinary Pathobiology, College of Veterinary Medicine, 250 McElroy Hall, Stillwater, OK 74078,
https://cvhs.okstate.edu/Veterinary_Pathobiology)

Spinal cord (left) heart (right), calf. In both tissues, there are coalescing areas of necrosis. (HE, 6X).

A large abscess was found at the base of the umbilicus. All lung lobes were wet and heavy and slightly reddened. An increased lobular pattern was noted in the cranioventral lung lobes.

The entire length of the spinal cord was sectioned and examined after fixation. A demarcated, regionally extensive, brown focus of malacia was found in the lumbar spinal cord. Other significant gross abnormalities were not observed in the rest of spinal cord segments or the brain.

Laboratory results: Hepatic vitamin E level and trace mineral analysis (including selenium) were all within normal limits. *Trueperella pyogenes* was recovered from the umbilical abscess.

Microscopic Description: Heart: Multifocal to confluent necrotic foci are randomly distributed in the myocardium. Cardiomyocyte degeneration and necrosis characterized by hypereosinophilia, fragmentation, pyknosis, karyorrhexis, and mineralization is widespread. Loss of cardiomyocytes and collapse of endomysium are accompanied by fibrosis and infiltrates of lymphocytes, macrophages, and few neutrophils. Small clusters (10-50 µm in diameter) of intracytoplasmic protozoal tachyzoites are commonly found in the cardiomyocytes and occasionally in Purkinje fibers at the periphery of necrotic foci or non-inflamed areas. Tachyzoites are basophilic, crescent-shaped, approximately 5 x 2 µm, with a prominent central nucleus. Spherical protozoal tissue cysts, measuring 10-20 µm in diameter are uncommonly seen containing a thin (< 1 µm), eosinophilic cyst wall and numerous tightly packed bradyzoites. Multiple Anichkov cells are observed within areas of necrosis and fibrosis.

Spinal cord: In the lumbar spinal cord, more than 70% of the parenchyma is obscured by regionally extensive necrosis and accompanying inflammatory infiltrates. Lesions center on the ventral sulcus and the gray matter, extending to the white matter, and are characterized by marked spongiosis, disruption and loss of neuropil, neuronal degeneration and loss, replaced by numerous foamy gitter cells, foci of gliosis, and scattered lymphocytes and plasma cells. Clusters of protozoal tachyzoites and tissue cysts are commonly identified within the neuropil (Figs. 3 & 5) and vascular endothelium (Fig. 4), and occasionally also found within glial cells and neurons. Multifocally, Virchow-Robin spaces and the leptomeninges are expanded by moderate numbers (2-5 layers) of lymphocytes and neutrophils. Endothelial cells are hypertrophic, and occasionally contain intracytoplasmic protozoal tachyzoites. Axonal degeneration with spheroids is prominent. The central canal is disrupted by inflammation and filled with proteinaceous fluid, neutrophils, lymphocytes, cellular debris and intralesional tachyzoites. The lining ependymal cells are attenuated or necrotic and lost.
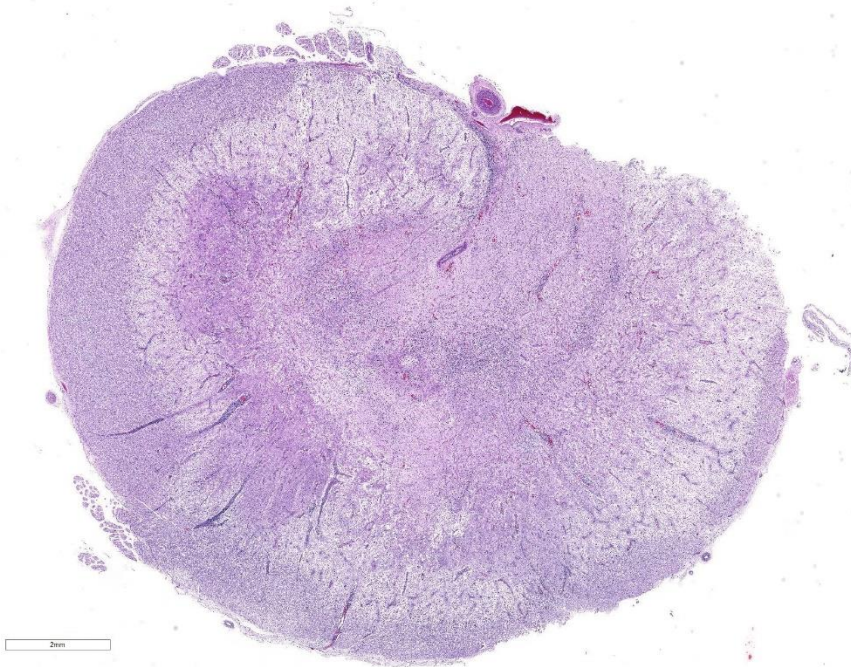
Spinal cord, calf. The degree of malacia within the spinal cord results in a lack of delineation between grey and white matter. (HE 10X)

Contributor's Morphologic Diagnosis:

Heart: Marked, chronic-active, multifocal to coalescing necrotizing myocarditis, lymphohistiocytic, with fibrosis, mineralization, abortive myocardial regeneration and intralesional protozoal tachyzoites and tissue cysts.

Lumbar spinal cord: Severe, subacute, multifocal and regionally extensive, necrotizing meningomyelitis, lymphohistiocytic and neutrophilic, with spongiosis, gliosis, perivascular cuffing, neuroaxonal degeneration and intralesional protozoal tachyzoites and tissue cysts.

Contributor's Comment: The microscopic findings are consistent with apicomplexan protozoal infection-associated myocarditis and meningomyelitis. The causative protozoans are confirmed as *Neospora caninum* by their characteristic ultrastructural features. Similar lesions and microorganisms were also identified in the skeletal muscles throughout the body, and to a lesser extent, in the brainstem and the cerebrum of this calf.

Neosporosis is a significant cause of abortion and stillbirth in both beef and dairy cattle worldwide.[1-5] The causative agent, *Neospora caninum*, is an apicomplexan protozoal parasite known as a major pathogen of cattle and dogs.[1-3] Abortion may occur from 3 months gestation to term with a peak at 5-6 months gestation in the affected cows.[2] Other than reproductive failure, *N. caninum* infection rarely causes clinical disease in adult cattle and calves.[1] However, occasionally, neurologic disease as a result of encephalomyelitis may occur in congenitally infected calves less than 4 months of age[2] and clinical signs such as ataxia, hyperextension of limbs, weakness and paralysis have been reported.[2,3,6,7,8]
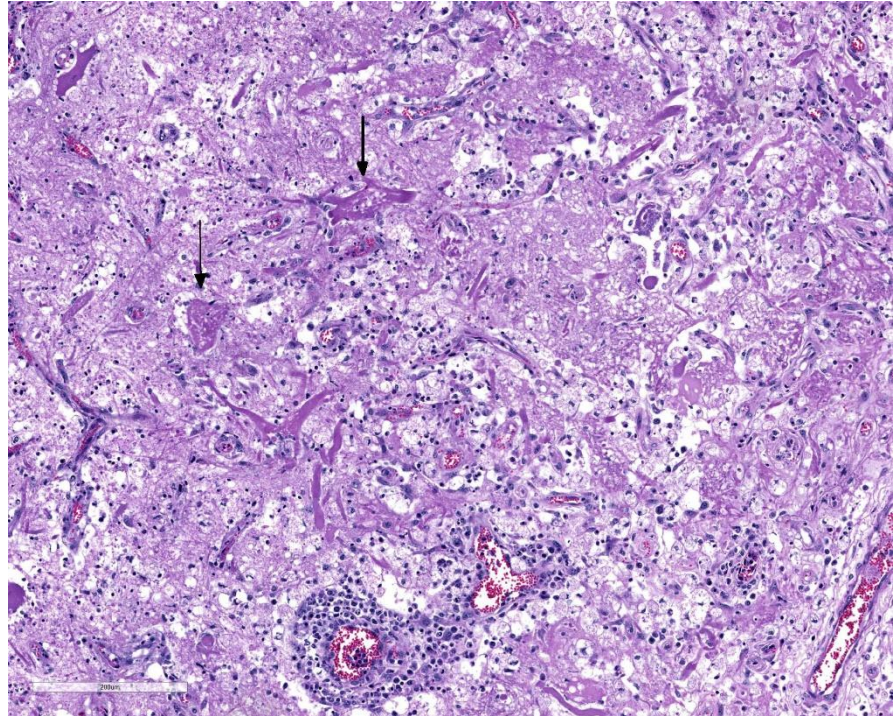
Dogs and several wild canids are the definitive hosts of *N. caninum*, whereas cattle and other warm-blooded animals serve as intermediate hosts.[1,5] The pathogenesis of *N. caninum* infection in cattle is not fully understood. Both transplacental and

horizontal transmissions play an important role in bovine neosporosis.[1,6] Transplacental transmission occurs when tissue cysts are reactivated in the persistently infected cow (endogenous) or when the oocysts are ingested by the naïve cow (exogenous).[1,6] *N. caninum* is transmitted efficiently from the pregnant cows to their offspring during pregnancy, and the consequences of infection include abortion, birth of a weak calf occasionally with neurologic signs, or


Spinal cord, calf. Within the malacic and edematous grey matter, there is ischemic necrosis of remaining neutrons. Vessels are often cuffed by multiple layers of neutrophils, macrophages, and lymphocytes. (HE 154X)

birth of a persistently infected but clinically healthy calf.[1,3] Abortion is believed to be a result of one or more of the following mechanisms: (1) primary parasite-induced placental damage; (2) fetal tissue damage due to parasite multiplication; (3) maternal immune expulsion of the fetus (Th1-type immunoresponse) due to *N. caninum* induced pro-inflammatory cytokines in the placenta.[1,3] Cow-to-cow transmission has not yet been proven.[1] The only demonstrated natural mode of postnatal infection in cattle is ingestion of sporulated *N. caninum* oocysts from the environment (e.g. contaminated canine feces).[9]

Neospora caninum is an intracellular protozoa and has three infectious stages, including sporozoites, tachyzoites and bradyzoites.[1] Sporozoites are present in

oocysts that are shed in the feces of the definitive host. Tachyzoites and bradyzoites are found in the tissues of both intermediate and definitive hosts.[1-3] Tachyzoites are rapidly dividing forms, crescent-shaped, approximately 6 x 2 µm with a centrally placed nucleus. They may infect a variety of cells including neural cells, vascular endothelial cells, myocytes, hepatocytes, renal cells, alveolar macrophages and placental trophoblasts.[1] Bradyzoites are slowly replicating forms present within the tissue cysts. They are slender, approximately 6.5 x 1.5 µm with a terminally located nucleus and contain several Periodic Acid Schiff positive amylopectin granules.[1] Tissue cysts found in infected calves are usually smaller (<50 µm in diameter) with thinner (<2 µm thick) walls compared to those in dogs (up to 107 µm in diameter).[1]
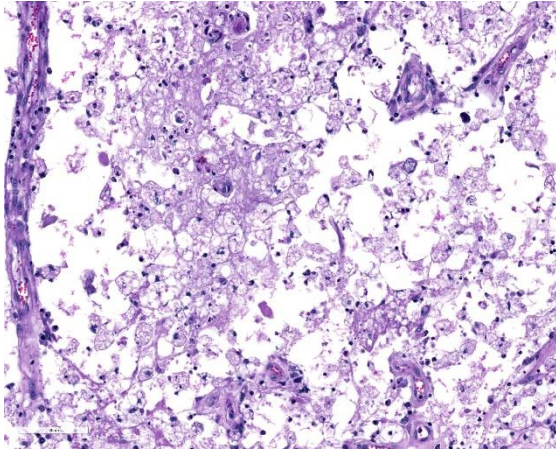
Spinal cord, calf. There are extensive areas of necrosis within deep white matter in all funiculi, with dilation and loss of myelin sheaths, enclosed nerve fibers, and replacement by numerous Gitter cells. (HE 273X)

In the current case, the lesions were most severe in the lumbar spinal cord, heart, and the skeletal muscles. Interestingly, the gross lesions somewhat resembled those of calves with vitamin E/selenium deficiency (white muscle disease), because of the widespread myonecrosis. However, neosporosis was confirmed on histopathology by demonstrating numerous *N. caninum* organisms. Minor lesions were also noted in the brainstem and cerebrum, characterized by foci of necrosis with gliosis, aggregates of mononuclear cells and prominent perivascular cuffing. Furthermore, the vitamin E and selenium levels were within normal limits in this calf.

Microscopically, abortifacient apicomplexan protozoans such as *N. caninum*, *Toxoplasma gondii*, and *Sarcocystis cruzi*, can be indistinguishable in HE stained sections.[2,5] *Toxoplasma gondii* is seen in rodents, dogs, cats, and human with CNS and reproductive diseases but it has not been proven to cause abortion in cattle.[2] A recent study

documented that some species of *Sarcocystis*, specifically *S. cruzi*, can cause neurologic disease in calves and adult cattle.[10] However, it was suggested that if apicomplexan-like protozoans are seen in the brain tissue of aborted calves, they can be assumed to be *N. caninum*.[2]

Ultrastructurally, *N. caninum*, *T. gondii*, and *S. cruzi* have different morphologies that can be distinguished from each other.[2,11] *N. caninum* contains 8-12 electron-dense rhoptries and numerous micronemes cranial to the nucleus, whereas *T. gondii* contains few (4-8) spongy or honeycomb-like rhoptries, few micronemes, and many micropores.[11] Individual merozoites of *S. cruzi* are smaller (3-5 x 2-3 µm) compared to the others and they have numerous micronemes but lack rhoptries.[2,10]

Immunohistochemistry staining is a useful tool to identify *N. caninum* organisms on histopathology slides, but false positives due to cross reactions to *T. gondii* have been
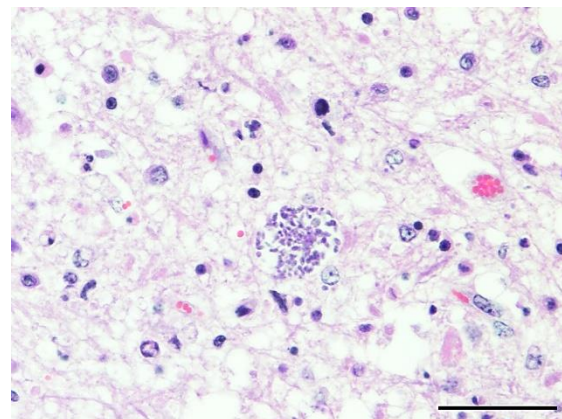
Spinal cord, calf. Tissue cysts containing numerous tachyzoites are present within cells within the neuropil. (HE 400X) (Photo courtesy of: Oklahoma State University, Department of Veterinary Pathobiology, College of Veterinary Medicine, 250 McElroy Hall, Stillwater, OK 74078, https://cvhs.okstate.edu/Veterinary_Pathobiology)
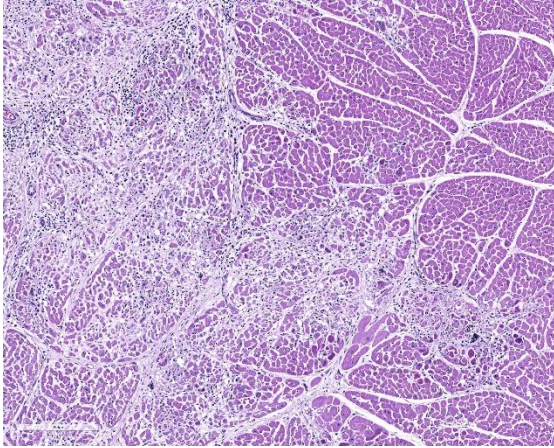
Heart, calf. The myocardium contains large, coalescing areas of necrosis and myofiber loss. (HE 128X)

reported in some studies.[2,12] PCR is another commonly used method for diagnosis and many PCR assays targeting different *N. caninum* genes have been published.[2,12] Serology is a practical tool to diagnose *N. caninum*-related abortions. It has an advantage of antemortem diagnosis of the disease and is commonly used as a screening test in herds.[2]

Contributing Institution:

Oklahoma State University
Department of Veterinary Pathobiology
College of Veterinary Medicine
250 McElroy Hall
Stillwater, OK 74078
https://cvhs.okstate.edu/Veterinary_Pathobiology

JPC Diagnosis: 1. Spinal cord, grey and white matter: Myelitis, necrotizing, multifocal to coalescing, severe with mild multifocal lymphohistiocytic and neutrophilic meningitis, and numerous intra- and extracellular apicomplexan zoites.

2. Heart: Myocarditis, necrotizing, subacute, multifocal to coalescing, marked,

with occasional intracellular apicomplexan zoites.

JPC Comment: The contributor has provided an excellent review of *Neospora*, a common finding in bovine abortion in many parts of the US. The comment is so well-constructed, that our comment in turn will focus on some lesser known, but interesting "facts" about *Neospora* that are often overlooked in its review.

While not an author on the original Norwegian paper by Bjerkas et al. describing *Neospora* as an "unidentified cyst-forming sporozoon" causing encephalomyelitis and myositis in three consecutive litters of dogs, a PubMed search for both "Neospora" and "Dubey" brings up an amazing 277 titles.

In the last thirty years, *Neospora caninum* has appeared eleven times in the Wednesday Slide Conference, (and a twelfth submission
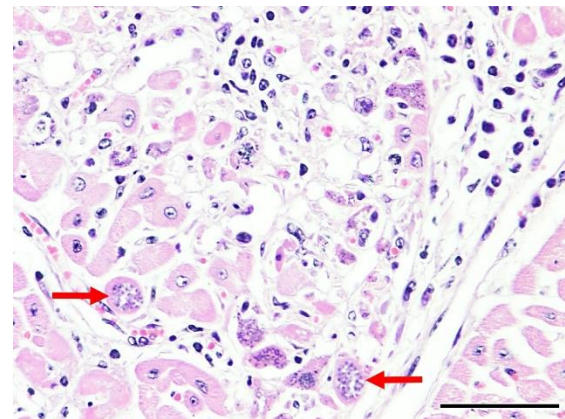
Heart, calf. Tissue cysts are present within cardiomyocytes as well. (HE 400X) (Photo courtesy of: Oklahoma State University, Department of Veterinary Pathobiology, College of Veterinary Medicine, 250 McElroy Hall, Stillwater, OK 74078, https://cvhs.okstate.edu/Veterinary_Pathobiology)
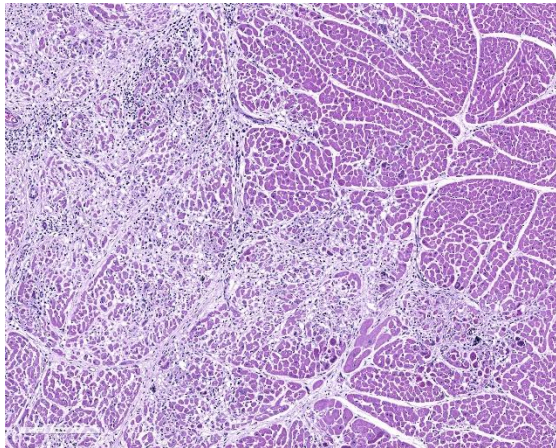
*Heart, calf. The myocardium contains large, coalescing areas of necrosis and myofiber loss. (HE 128X)*

was diagnosed as *Sarcocystis* by Dr. J.P. Dubey based on ultrastructural analysis and later, immunohistological confirmation). In the WSC, it has actually been submitted more often in the dog, from the brain (4), spinal cord (3), skin (2) and skeletal muscle (1). In the ox, this will be the second case in the spinal cord, and the first submission of the heart lesion; a previously presented case was diagnosed in the brainstem.

In addition to the very characteristic infections in intermediate hosts such as cattle and dogs (dogs also serve as the definitve host), it has also been found in aberrant hosts (usually singular cases) to include sheep, water buffalo, horses, goats, white-tailed deer, a raccoon, and a rhinoceros. Dr. Dubey stresses that simply finding DNA of *N. caninum*, or antibodies to the organism, is not synonymous with identiifying the viable apicomplexan parasite histologically. Serologic positivity to *N. caninum* has been well documented in humans, but disease has not.[13]

Dubey et al considers *N. caninum* to be one of the most "efficiently transplacentally transmitted parasites among all known microbes in cattle," with all calves in some herds being born infected but asymptomatic.[13] In some parts of the US, it is such a common cause of abortion in calves that, even in the absence of finding characteristic tissue cysts, the presence of glial nodules in the brain and areas of necrosis in the heart or liver is considered adequate proof of its etiology. Cow-to-cow (horizontal) transmission has not been established.[14] While previously identified in the CNS of adult horses, a recent publication documents the presents of *Neospora* tachyzoites in the lung, liver and heart of an equine abortus, suggesting that *N. caninum* should now be considered as an uncommon

Heart, calf. Electron micrography of the apicomplexan zoites demonstrates multiple rhoptries (arrow) and numerous micronemes (arrowhead). (Photo courtesy of: Oklahoma State University, Department of Veterinary Pathobiology, College of Veterinary Medicine, 250 McElroy Hall, Stillwater, OK 74078,
https://cvhs.okstate.edu/Veterinary_Pathobiology)
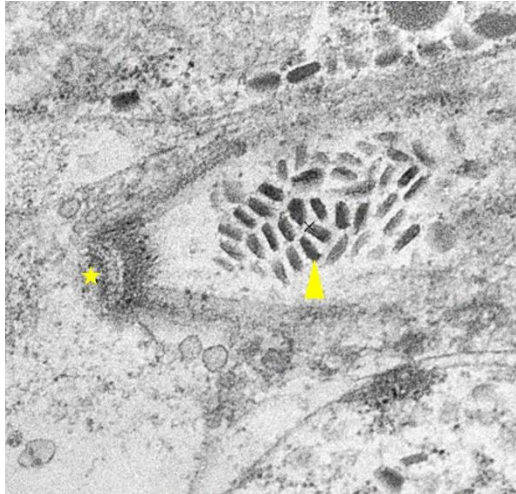
Heart, calf. Electron micrography of the apicomplexan zoites demonstrates a conoid ring (star) and numerous micronemes (arrowhead). (Photo courtesy of: Oklahoma State University, Department of Veterinary Pathobiology, College of Veterinary Medicine, 250 McElroy Hall, Stillwater, OK 74078, https://cvhs.okstate.edu/Veterinary_Pathobiology)

cause of equine abortion as well. [15]

References:

1. Dubey JP, Buxton D, Wouda W. Pathogenesis of bovine neosporosis. *J Comp Pathol*. 2006;134(4):267-289.

2. Dubey JP, Schares G. Diagnosis of bovine neosporosis. *Vet Parasitol*. 2006;140(1-2):1-34.

3. Innes EA, Wright S, Bartley P, et al. The host-parasite relationship in bovine neosporosis. *Vet Immunol Immunopathol*. 2005;108(1-2):29-36.

4. Helman RG, Stair EL, Lehenbauer TW, et al. Neosporal abortion in Oklahoma cattle with emphasis on the distribution of brain lesions in aborted fetuses. *J Vet Diagn Invest*. 1998;10(3):292-295.

5. Dubey JP, Schares G. Neosporosis in animals--the last five years. *Vet Parasitol*. 2011;180(1-2):90-108.

6. Marugan-Hernandez V. *Neospora caninum* and Bovine Neosporosis: Current Vaccine Research. *J Comp Pathol*. 2017;157(2-3):193-200.

7. Uesaka K, Koyama K, Horiuchi N, et al. A clinical case of neosporosis in a 4-week-old holstein friesian calf which developed hindlimb paresis postnatally. *J Vet Med Sci*. 2018;80(2):280-283.

8. De Meerschman F, Focant C, Detry J, et al. Clinical, pathological and diagnostic aspects of congenital neosporosis in a series of naturally infected calves. *Vet Rec*. 2005;157(4):115-118.

9. McCann CM, McAllister MM, Gondim LFP, et al. *Neospora caninum* in cattle: Experimental infection with oocysts can result in exogenous transplacental infection, but not endogenous transplacental infection in the subsequent pregnancy. *International Journal for Parasitology*. 2007;37(14):1631-1639.

10. Dubey JP, Calero-Bernal R, Verma SK, et al. Pathology, immunohistochemistry, and neurological sarcocystosis in cattle. *Vet Parasitol*. 2016;223:147-152.

11. Lindsay DS, Speer CA, Toivio-Kinnucan MA, et al. Use of infected cultured cells to compare ultrastructural features of *Neospora caninum* from dogs and *Toxoplasma gondii*. *Am J Vet Res*. 1993;54(1):103-106.

12. van Maanen C, Wouda W, Schares G, et al. An interlaboratory comparison of immunohistochemistry and PCR methods for detection of *Neospora caninum* in bovine

foetal tissues. *Vet Parasitol*. 2004;126(4):351-364.

13. Dubey JP, Schares G, Ortega-Mora LM. Epidemiology and control of neosporosis and Neospora caninum. *Clin Microbiol Rev* 2007; 20(2):323-367.

14. Dubey JP. Review of *Neospora caninum* and neosporosis in animals. *Korean J Parasit* 2003; 41(1):1-16.

15. Anderson JA, Alves DA, Cerquieira-Cezar CK, da Silva AF, Murata FHA, Norris JK, Howe DK, Dubey JP. Histologically, immunohistochemically, ultrastructurally, and molecularly confirmed neosporosis abortion in an aborted equine fetus. *Vet Parasit* 2019; 270:20-24.

CASE II: 18-0311 (JPC 4136399).

Signalment: 4-year-old male castrated mixed breed dog (*Canis familiaris*)

History: One year prior to euthanasia, the patient began exhibiting bruxism in periods of stress. This worsened to more frequent periods of anxiety and loud bruxism persisting for hours. Five months prior to euthanasia (seven months after onset of clinical signs), the patient became hyperreactive to stimuli around the face and head, showed unclassified ataxia and balance problems, and began to walk into objects. On presentation to the Neurology Service at the university, the patient had vestibular/cerebellar ataxia and an inconsistent menace response bilaterally. Fundic examination was normal. The MRI report stated that the cerebrum had widened cerebral sulci, a severely dilated ventricular system, and small basal nuclei, thalamus, and cerebellum with prominent folia. The patient's clinical signs continued to

Brain, dog. Multiple cross sections demonstrate marked atrophy of the cerebral and cerebellar cortex, with hydrocephalus ex vacuo. (Photo courtesy of: University of Pennsylvania School of Veterinary Medicine, Department of Pathobiology, http://www.vet.upenn.edu/research/academic-departments/)

progress, and euthanasia was elected due to quality of life concerns.

Gross Pathology: The cerebral cortex was severely atrophied with widening of the sulci and secondary dilation of the lateral ventricles (hydrocephalus). The cerebellum appears slightly small. No additional abnormalities were detected on gross examination.

Laboratory results: None

Microscopic Description:

Sections of cerebellum or cerebellum with brainstem are submitted. The cerebellar cortex is mildly diffusely atrophied, with slight thinning and marked pallor of the cerebellar folia. Within the folia, there is marked loss of neurons within the granule cell layer, with fine vacuolation of the remaining parenchyma. Purkinje cells are irregularly spaced, with scattered necrosis and loss. Neurons and glial cells frequently contain abundant pale eosinophilic cytoplasmic storage material that has a globular or granular appearance. The material often peripheralizes the nucleus and variably distends the perikaryon. Affected neurons are degenerate, with cytoplasmic

Cerebellum, dog. The cerebellar folia (top and left) are markedly thin and hypocellular. The granular layer is indistinct. (HE, 8X)

swelling and central chromatolysis. The neuroparenchyma is mildly hypercellular, with increased numbers of glial cells, predominately microglia. Similar changes are detected in neurons throughout the entire central nervous system (cerebral cortex, cerebellum, brainstem nuclei, and spinal cord grey matter) and retina (slides not submitted).

Histochemical stains are applied to multiple sections of central nervous system tissue (see photomicrographs). The cytoplasmic storage material stains magenta with Periodic acid-Schiff (PAS) and is positive with Luxol fast blue.

### Contributor's Morphologic Diagnosis:

Cerebellum: Severe chronic neuronal degeneration and loss with abundant intracytoplasmic storage material and cortical atrophy

Contributor's Comment: Although the recognition of intracellular storage material can be relatively straightforward, definitive identification of the material and subsequent categorization of the storage disease can pose a diagnostic challenge for veterinary pathologists. In this case, an extensive histologic survey of the major organs identified intracytoplasmic pigment only in the central nervous system (CNS) and retina, with the neurons most severely affected. The microscopic appearance, histochemical staining pattern, and cellular distribution of the pigment are most consistent with a type of neuronal ceroid lipofuscinosis (NCL), although definitive diagnosis requires electron microscopy and/or genetic testing.[3,6,13]

NCLs are neurodegenerative diseases characterized by the accumulation of lipopigment material within cells, always and most severely affecting neurons.[3] Like other lysosomal storage diseases, a mutation in a protein (typically an enzyme) critical to the metabolic pathway of digesting a material leads to accumulation of the now indigestible material in residual bodies, gradually leading to cell dysfunction and death.[6,20] More than 360 mutations in over a dozen genes have been identified as causes of these diseases in humans[8,20,21], dogs[1,2,9,10,13], sheep[22], pigs[4], horses[23], goats[7], and cattle[10]. NCL has been described in cats, although a genetic cause has not been identified in this species.[5] The vast majority of mutations are within genes coding for lysosomal enzymes, although endoplasmic reticulum and Golgi apparatus proteins have also been implicated.[13,15,16,20,21]

The accumulated ceroid-lipofuscin lipopigment in NCL is similar to both ceroid and lipofuscin but is not truly a variant of
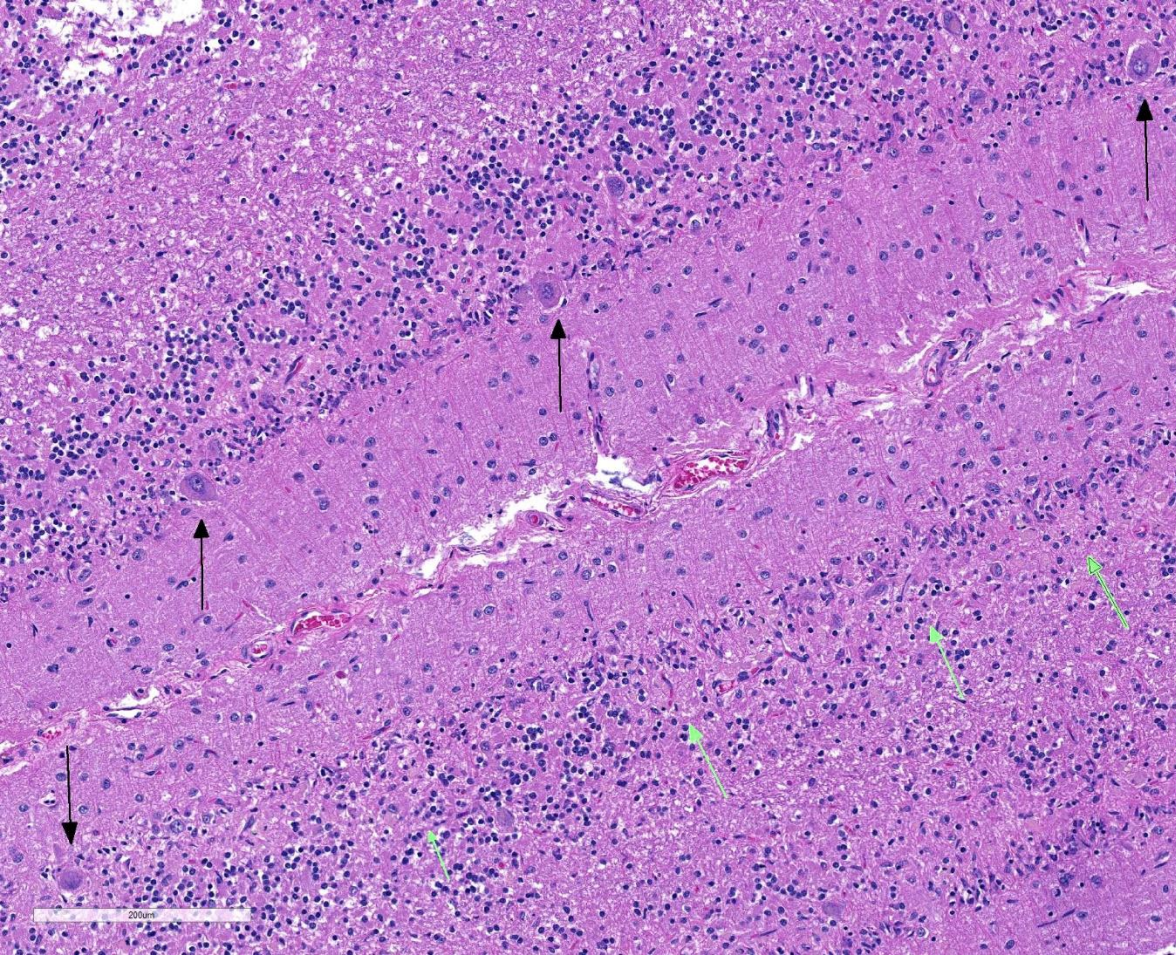
Cerebellum, dog. There is marked loss of Purkinje cells with a very prominent stretch of hypocellular granular layer without any overlying Purkinje cells at bottom right (green arrows) (HE, 163X)

either. Ceroid is a pigment that accumulates within cells due to a pathological process, such as a nutritional deficiency. Lipofuscin is also a pigment that accumulates within post-mitotic cells with age as a "wear-and-tear" material. The NCL lipopigment is composed primarily of protein with lesser lipid components.[13,15] The specific protein component is determined by mutation, but is typically derived from subunit C of mitochondrial ATP synthase[13], or less commonly from a sphingolipid activator protein.[18,20]

Ceroid-lipofuscin is yellow-gold to lightly eosinophilic on H&E staining. In cases of NCL, there are globular or botryoid accumulations within the axon hillock that displace the nucleus and Nissl substance. The material stains positively with PAS and Luxol fast blue stains and is variably acid-fast positive.[3] Ultrastructurally, the lipopigment has characteristic "curvilinear" or "fingerprint bodies" approximately 15 nm in diameter.[3,6,13,20] The material will autofluoresce under ultraviolet light, particularly in unstained paraffin-embedded tissue sections[13,15]

Neurons throughout the CNS are always affected, although the material may also accumulate in neurons of the peripheral nervous system neurons (e.g. in the intestinal plexi) as well as other cells in the CNS, including astrocytes, oligodendrocytes, and microglia. Later in

disease, cells in tissues outside of the nervous system may also accumulate storage material, including hepatic Kupffer cells and epithelial cells in the kidneys, pancreas, lungs, reproductive organs, skin, endocrine organs, salivary glands, etc.[13,16,20]

Affected individuals show progressive cognitive decline, visual and motor deficits, and seizures.[13,14] Age of onset can vary greatly, with most affected animals showing signs early in life, however there are late forms as well.[6,15] The disease is invariably fatal, with death occurring within months or up to a few years after clinical signs first present.[3,20]
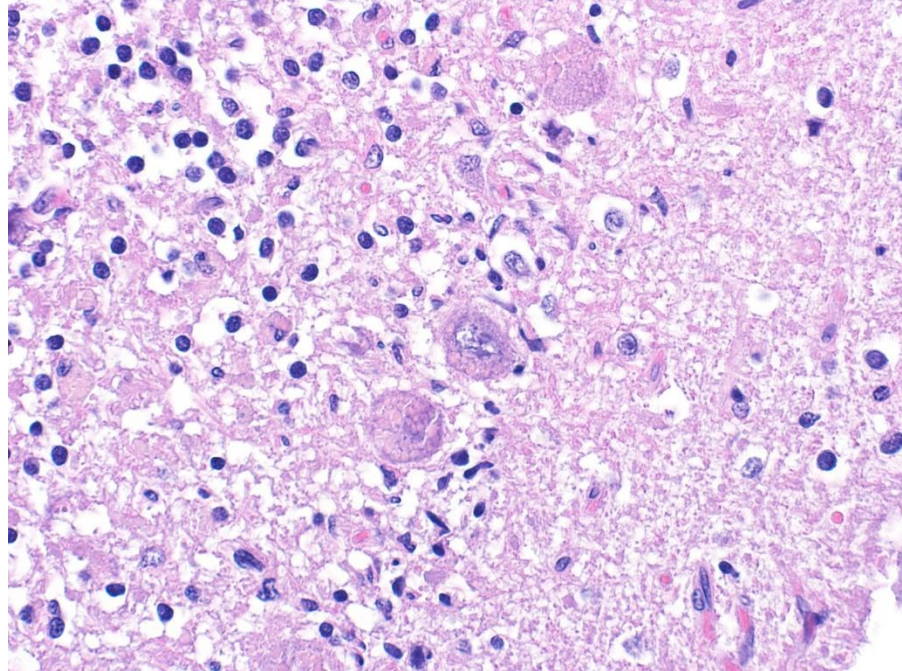

Cerebellum, dog. Remaining Purkinje cells contain numerous intracytoplasmic vacuoles containing a tan-pink granular material (ceroid). Glial cells/macrophages in the adjacent granular layer also contain similar material in their cytoplasm. (HE, 400X)   (Photo courtesy of: University of Pennsylvania School of Veterinary Medicine, Department of Pathobiology, http://www.vet.upenn.edu/research/academic-departments/)

Contributing Institution:

University of Pennsylvania
School of Veterinary Medicine
Department of Pathobiology
http://www.vet.upenn.edu/research/academic-departments/

JPC Diagnosis: Cerebellum: Neuronal degeneration, necrosis, and loss, diffuse, severe, with marked neuronal intracellular granular pigment accumulation, gliosis, and neuronophagia.

**JPC Comment**: The contributor has provided an excellent review of neuronal-ceroid lipofuscinosis in animals.

The disease was first described in humans by Dr. Otto Christian Stengel in Germany as a juvenile onset disorder resulting in blindness and progressive dementia. In 1902, English neurologist and pediatrician Frederick Eusace Batten described a similar disorder in two members of the same family, but was also the first to describe the neuropathology of cerebral and ocular macular degeneration, and it is from this investigator that the disease was called Batten's disease for many years (with that term now being restricted to certainly particular forms of the disease).[18]

Today, at least 14 affected genes have been implicated in NCL (neuronal ceroid-lipofuscinosis), which result in various manifestations that may appear in infants, toddlers, juveniles, and adult onset form. Eight of these 14 genes have been identified
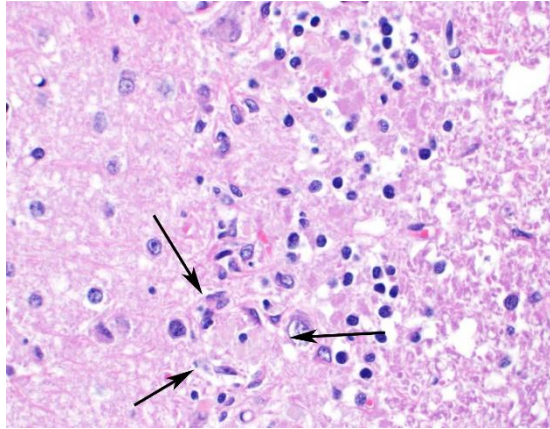
Cerebellum, dog. Within the Purkinje cell layer, there are neuronophagic nodules (arrows) populated by glial cells and macrophages containing abundant phagocytosed ceroid from effete Purkinje cells. (HE, 400X)

in canine CNL, as noted in Table 1, below.[12] A number of schemes are used in the classification of NCLs in humans, to include the historical schema, largely based on onset, a classification scheme based on abnormal genes and accumulated proteins, and one based on typical ultrastructural findings and abnormal enzymatic activities. A review of these classifications and a very good overall review of the disease in

general in humans is available by Nita et al. below.[18]

Although there are a wide diversity of mutated genes, affected proteins, and manifestations, the NCLs are traditionally grouped together due to the common presence of autofluorescent pigment accumulation within neurons and other cells. Like many lysosomal storage diseases, many of the identified abnormal gene products in the variants of NCL accumulate in lysosomes, as do ceroid lipoportain pigments. While early attempts at classification assumed that the appearance of inclusions were specific for each variant, more recent investigation has shown that they are not specific for each disease, may vary with tissue examined, and the same NCL may include more than one pattern of inclusion.[18]

References:

1. Awano T, Katz ML, O'Brien DP, Sohar I, et al. A frame shift mutation in canine TPP1 (the ortholog of human CLN2) in a juvenile Dachshund with neuronal ceroid

Table 1

Summary of canine NCL-associated disease sequence variants.[a]

Disease	Gene	Sequence variant	Amino acid change	Affected dog breed
CLN1	PPT1	c.736_737insC	p.F246Lfs*29	Dachshund [20]
CLN1	PPT1	c.124 + 1G > A	Splice variant	Cane Corso [12]
CLN2	TPP1	c.325delC	p.A108Pfs*6	Dachshund [21]
CLN5	CLN5	c.619C > T	p.Q207X	Border Collie [19]
				Australian Cattle Dog [14]
				Mixed breed [5,18]
CLN5	CLN5	c.934_935delAG	p.E312Vfs*6	Golden Retriever [22]
CLN6	CLN6	c.829T > C	p.W277R	Australian Shepherd [23]
CLN7	MFSD8	c.491T > C	p.F282Lfs*13	Chinese Crested [13]
				Chihuahua [24,25]
CLN8	CLN8	c.491T > C	p.L164P	English Setter [15]
CLN8	CLN8	c.585G > A	p.W195X	Australian Shepherd & Australian Cattle Dog [17]
				German Shorthaired Pointer[b]
CLN8	CLN8	g.30852988_30902901del	CLN8 absence	Alpenländische Dachsbracke [26]
CLN8	CLN8	c.349dupT	p.Glu117*	Saluki [6]
CLN10	CTSD	c.597G > A	p.M199I	American Bulldog [27]
CLN12	ATP13A2	c.1623delG	p.P541 fs*56	Tibetan Terrier [28]
CLN12	ATP13A2	c.1118C > T	p.Thr373Ile	Australian Cattle Dog [29]

[a] Updated from previous published list [5].
[b] This report.

(Reprinted from reference 12).

lipofuscinosis. Molec Genet Metab. 2006; 89: 254-260.

2. Awano T, Katz ML, O'Brien DP, Taylor JF, et al. A mutation in the cathepsin D gene (CTSD) in American bulldogs with neuronal ceroid lipofuscinosis. Molec Genet Metab. 2006; 87: 341-348.

3. Cantile C, Youssef, S. Nervous system. In: Maxie MG, ed. Jubb, Kennedy, and Palmer's Pathology of Domestic Animals. Vol 1. 6th ed. St. Louis, MO: Saunders Elsevier; 2016: 290-292.

4. Cesta MF, Mozzachio K, Little PB, Olby NJ, Sills RC, Brown TT. Neuronal ceroid lipofuscinosis in a Vietnamese pot-bellied pig (Sus scrofa). Vet Pathol. 2006;43(4):556-560.

5. Chalkley MD, Armien AG, Gilliam DH, Johnson GS, Zeng R, Wünschmann A, Kovi RC, Katz ML. Characterization of neuronal ceroid-lipofuscinosis in 3 cats. Vet Pathol. 2014;51(4):796-804.

6. Ferreira CR, Gahl WA. Lysosomal Storage Diseases. Translational Science of Rare Diseases. 2017; 2: 1–71.

7. Fiske RA, Storts RW. Neuronal ceroid-lipofuscinosis in Nubian goats. Vet Pathol. 1988; 25: 171-173.

8. Gao HL, Boustany RMN, Espinola JA, Cotman SL, et al. Mutations in a novel CLN6-encoded transmembrane protein cause variant neuronal ceroid lipofuscinosis in man and mouse. Am J Hum Genet. 2002; 70: 324-335.

9. Goebel HH, Bilzer T, Dahme E, Malkusch F. Morphological studies in canine (Dalmatian) neuronal ceroid-lipofuscinosis. Am J Med Genet Suppl. 1988; 5: 127-139.

10. Guo J, Johnson GS, Brown HA, Provencher ML. A CLN8 nonsense mutation in the whole genome sequence of a mixed breed dog with neuronal ceroid lipofuscinosis and Australian shepherd ancestry. Molec Genet Metab. 2014; 112: 302-309.

11. Guo J, Johnson GS, Cook J, Harris OK, Mhlanga-Mutangadura T, Schabel RD, Jensen CA, Katz ML. Neuronal ceroid lipofuscinosis in a German Shorthaired Pointer associated with a previously reported CLN8 nonsense variant. *Mol Gen Metabol Rep* 2019; 21. Https://doi.org/10.1016/j.ymgm4.2019.100521.

12. Harper PAW, Walker KH, Healy PJ, Hartley WJ, et al. Neurovisceral ceroid-lipofuscinosis in blind Devon cattle. Acta Neuropathologica. 1988; 75: 632-636.

13. Jolly RD, Palmer DN, Studdert VP, Sutton RH, et al. Canine ceroid-lipofuscinoses: A review and classification. Journal of Small Animal Practice. 1994; 35: 299-306.

14. Katz ML, Narstrom K, Johnson GS, O'Brien DP. Assessment of retinal function and characterization of lysosomal storage body accumulation in the retinas and brains of Tibetan terriers with ceroid-lipofuscinosis. Am Jour Vet Research. 2005; 66:67-76.

15. Katz ML, Rustad E, Robinson GO, Whiting REH, Student JT, Coates JR, Narfstrom K. Canine neuronal ceroid lipofuscinoses: Promising models for preclinical testing of therapeutic interventions. Neurobiology of Disease. 2017; 108: 277-287.

16. Melville SA, Wilson CL, Chiang CS, Studdert VP. A mutation in canine CLN5 causes neuronal ceroid

lipofuscinosis in border collie dogs. Genomics. 2005; 86: 287-294.

17. Nakamoto Y, Yamato O, Uchida K, Nibe K. Neuronal Ceroid-Lipofuscinosis in longhaired chihuahuas: Clinical, pathologic, and MRI findings. J Am Anim Hosp Assoc. 2011; 47: E64-E70.

18. Nita DA, Mole SE, Minassian BA. Neuronal ceroid lipofuscinoses. *Epileptic Disord* 2016; 18(Supple 2):S73-S88.

19. Palmer DN, Tyynela J, vanMil HC, Westlake VJ, Jolly RD. Accumulation of sphingolipid activator proteins (SAPs) A and D in granular osmiophilic deposits in miniature schnauzer dogs with ceroid-lipofuscinosis. J Inherit Metab Dis. 1997; 20: 74-84.

20. Pastores GM, Maegawa GHB. Neuropathic Lysosomal Storage Disorders. Neurol Clin. 2013 November; 31(4): 1051–1071.

21. Sun, A. Lysosomal storage disease overview. Ann Transl Med 2018; 6(24):476.

22. Tammen I, Houweling PJ, Frugier T, Mitchell NL, et al. A missense mutation (c. 184C > T) in ovine CLN6 causes neuronal ceroid lipofuscinosis in Merino sheep whereas affected South Hampshire sheep have reduced levels of CLN6 mRNA. Biochim Biophys Acta. 2006;1762: 898-905.

23. Url A, Bauder B, Thalhammer J, Nowotny N, et al. Equine neuronal ceroid lipofuscinosis. Acta Neuropathologica. 2001; 101: 410-414.

CASE III: KSU VDL (JPC 4032559).

Signalment: 4-month-old female Hereford bovine calf.

History: The calf presented to the referring DVM with opisthotonus, head tilt, and ataxia. The calf was treated with tulathromycin (Draxxin) and dexamethasone for suspected otitis. Amprolium and sucralfate were given for 5 days for suspected nervous coccidiosis. The calf was presented to KSU teaching hospital a month later in sternal recumbency and was unable to stand. The physical examination revealed bilateral dorsolateral strabismus, variable nystagmus, and positive pupillary, menace, and palpebral reflexes with strong tongue tone. The ear exam was normal. There was no response to oxytetracycline, thiamine and dexamethasone. The calf was not eating or drinking and occasionally took few sips of water. The calf was euthanized.
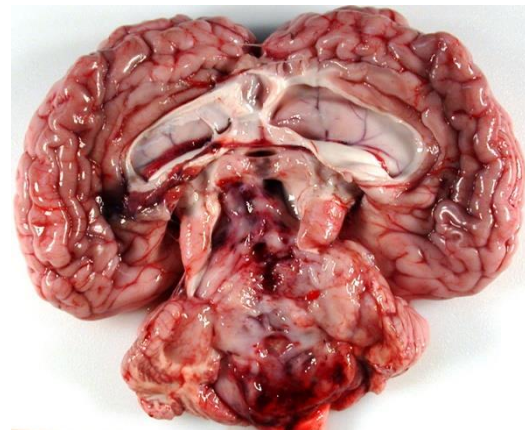
Cerebellum, calf. The fourth ventricle is replaced and expanded by a friable, pale white mass with multifocal hemorrhages. The mass extends into and occludes the mesencephalic aqueduct. Both lateral ventricles are markedly dilated.   (Photo courtesy of: Department of Diagnostic Medicine and Pathobiology, Kansas State Veterinary College of Veterinary Medicine, 1800 Denison Avenue, Manhattan, KS 66506 http://www.vet.k-state.edu/depts/dmp/index.htm)
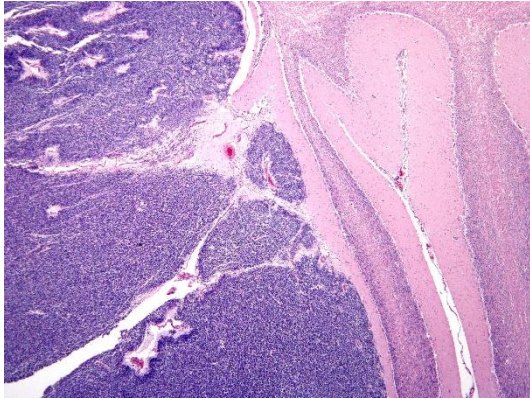
Cerebellum, calf. Subgross view of neoplastic cells compressing and peripherally invading the cerebellum. (Photo courtesy of: Department of Diagnostic Medicine and Pathobiology, Kansas State Veterinary College of Veterinary Medicine, 1800 Denison Avenue, Manhattan, KS 66506 http://www.vet.k-state.edu/depts/dmp/index.htm)

Gross Pathology: The calf was in good body condition. A soft, friable, gelatinous, pale white mass completely filled and expanded the fourth ventricle and compressed the cerebellar vermis and extended cranially and occluded the mesencephalic aqueduct. The lateral ventricles were markedly distended with cerebrospinal fluid that was pale yellow and cloudy. Multifocally, mild to moderate hemorrhages were present within the mass.

**Laboratory results:** None

Microscopic Description:

Brain: Expanding the fourth ventricle, compressing and superficially invading the brainstem and cerebellum is a moderately well-delineated, unencapsulated, highly cellular neoplasm composed of round to fusiform cells arranged in sheets supported by a scant fibrovascular stroma. Frequently, three to five cell-layer thick neoplastic cells also palisade around the capillaries (pseudorosettes). Occasionally, the cells palisade around a central fibrillar material (rosettes). The cells have scant eosinophilic cytoplasm and oval to elongate nuclei containing coarsely stippled chromatin and 1-4 nucleoli. There are 10 mitotic figures in ten 400X fields. The cells have variably distinct borders and there is mild anisocytosis and anisokaryosis. Within the neoplasm there are multifocal areas of necrosis, hemorrhage and a few lymphocytic infiltrates.

Histochemical stains are applied to multiple sections of central nervous system tissue (see photomicrographs). The cytoplasmic storage material stains magenta with Periodic acid-Schiff (PAS) and is positive with Luxol fast blue.

Contributor's Morphologic Diagnosis:

Brain, cerebellum and brainstem: Medulloblastoma with bilateral marked hydrocephalus of lateral ventricles.
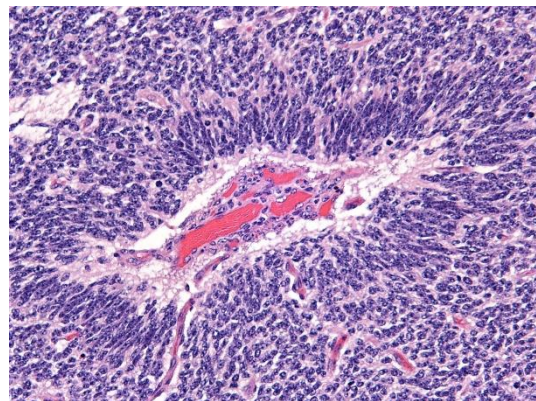
Cerebellum, calf. Neoplastic cells palisade around capillaries (pseudorosettes). (Photo courtesy of: Department of Diagnostic Medicine and Pathobiology, Kansas State Veterinary College of Veterinary Medicine, 1800 Denison Avenue, Manhattan, KS 66506 http://www.vet.k-state.edu/depts/dmp/index.htm)

Contributor's Comment:

Medulloblastoma is a malignant brain tumor that is thought to arise from an undifferentiated germ cells found below the pia mater during fetal and neonatal life.[2,11] The terminology medulloblastoma is exclusively used to indicate embryonal tumors arising in the cerebellum while similar neoplasms in other locations of the brain are called primitive neuroectodermal tumors (PNET).[2] In animals, it is reported in calves[5], young dogs[12], cats[7], baboons[1] and rats[9]. Medulloblastomas occur more frequently in children (80 %) and is the second most common malignant tumor in the central nervous system of children.[5]. In children, the neoplasm arises from the vermis and in adults it is located in cerebellar hemisphere. In humans, these neoplasms are seen more commonly in males but no such sex predisposition has been reported in animals.[2]

Medulloblastomas are malignant tumors that can invade into adjacent neuropil and disseminate via cerebrospinal fluid (CSF). Grossly, medulloblastomas are soft, friable, gray masses that arise from the cerebellum and expand the fourth ventricle. The neoplasm can obstruct the ventricles leading to obstructive hydrocephalus. Microscopically, the cells are round to polygonal, forming sheets or bands with scant cytoplasm and an elongated nucleus sometimes resembling a 'carrot'. Occasionally, the neoplastic cells can form Homer Wright and Flexner-Wintersteiner-like rosettes.[2,8]

There is variability in the immunohisto-chemical staining characteristics of cells
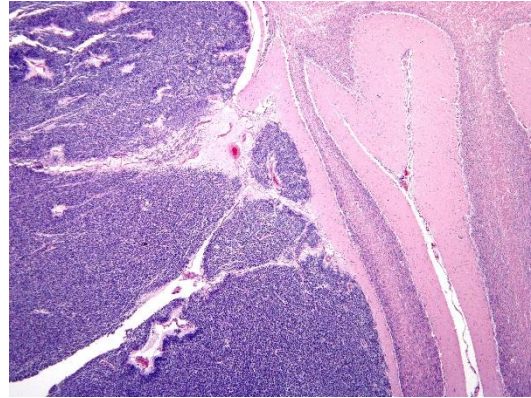
Cerebellum, calf. Neoplastic cells surrounding a central fibrillar material (Homer Wright rosettes). (Photo courtesy of: Department of Diagnostic Medicine and Pathobiology, Kansas State Veterinary College of Veterinary Medicine, 1800 Denison Avenue, Manhattan, KS 66506 http://www.vet.k-state.edu/depts/dmp/index.htm)

owing to the stages of differentiation. In one study of canine medulloblastoma, primitive neuroepithelium stained for vimentin and S-100; differentiated neurons stained for neuron specific enolase (NSE) and synaptophysin; differentiated astrocytes labeled positive for glial fibrillary acidic protein (GFAP), vimentin, NSE, and neurofilament.[12] In addition, the telomerase activity and c-kit expression were recently reported in canine medulloblastomas.[9]

Immunohistochemistry was performed in the current case for NSE, synaptophysin, GFAP, vimentin, cytokeratin, and S-100. The neoplastic cells were immunopositive for vimentin and S-100 and negative for GFAP, NSE, synaptophysin and cytokeratin, suggesting that the neoplastic cells are undifferentiated. Differentiation along neuronal and glial lineage is less common in animals than in humans.[2]
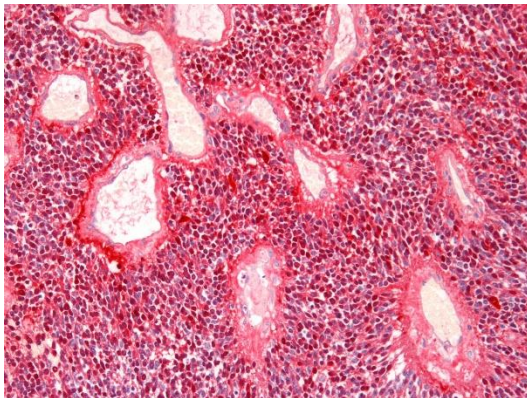
Contributing Institution:

Department of Diagnostic Medicine and
Pathobiology
Kansas State Veterinary College of
Veterinary Medicine
1800 Denison Avenue
Manhattan, KS 66506
http://www.vet.k-
state.edu/depts/dmp/index.htm

JPC Diagnosis: Cerebellum: Primitive
neuroectodermal tumor (medulloblastoma).

JPC Comment: Medulloblastoma is a
form of primitive neuroepithelial tumor that
likely arises from the external germinal cell
zone, which lies directly beneath the
meninges in the developing cerebellum.[6]
Normally, during fetal development,
cerebellar granular cells develop in the
external germinal zone then migrate past
Purkinje cells to form the granule cell layer.

Activation of the hedgehog pathway has
been shown not only to regulate normal
growth, but is also involved in the
tumorigenesis of several neoplasms,
including medulloblastomas.[4] More

*Cerebellum, calf. Neoplastic cells are immunopositive
for S-100.   (Photo courtesy of: Department of
Diagnostic Medicine and Pathobiology, Kansas State
Veterinary College of Veterinary Medicine, 1800
Denison Avenue, Manhattan, KS 66506
http://www.vet.k-state.edu/depts/dmp/index.htm)*

specifically, the Patched gene (*Ptc*) controls
growth and pattern formation in early neural
development and the adult cerebellum.[3] *Ptc*
gene encodes a Sonic hedgehog (*Shh*)
receptor and a tumor suppressor protein.
While many subtle aspects of signaling have
not been completely elucidated, it is clear
that a complex interaction between *Shh* and
Ptc is required for normal development. Shh
binds to Ptc, activates smoothened (*Smo*)
which leads to over expression of *Gli-1* and
some *Wnt* and *TGF-ß* gene families.[3,4]
(Hedgehog effectors *Gli-1* and *BclII* have
also been shown to be overexpressed in
medulloblastomas).[3] *Ptc*-knockout mice
(which allow for unregulated expression of
Shh target genes have a high incidence of
PNET formation – eight percent of *Ptc*-
heterozyogous mice develop tumors as early
as 5 weeks.[6] Tumor incidence increases
with age in *Ptc*-heterozygous mice with an
incidence of about 30% at six months of
age.[6] In humans, *Ptc* mutation has been
associated with basal cell carcinoma,
fibroma, medulloblastoma and
rhabdomyosarcoma.[4]

References:

1. Berthe J, Barneon G, Richer G, Mazue G.
   Medulloblastoma in a baboon (*Paio
   paio*). *Lab Anim Sci.* 1980; 30: 703-705.

2. Cummings J, de Lahunta A. *Veterinary
   Neuropathology,* Mosby, St. Louis, MO,
   1995; 378-379.

3. Goodrich LV, Milenković L, Higgins
   KM, Scott MP: Altered neural cell fates
   and medulloblastoma in mouse patched
   mutants. Science 277:1109-1113, 1997

4. Hahn H, Wojnowski L, Specht K,
   Kappler R, Calzada-Wack J, Potter D,
   Zimmer A, Müller U, Samson E,

Quintanilla-Martinez L, Zimmer A: Patched target Igf2 is indispensable for the formation of medulloblastoma and rhabdomyosarcoma. J Biol Chem 275:28341-28344, 2000

5. Jolly RD, Alley MR. Medulloblastoma in calves: A report of three cases. *Vet Pathol.* 1969; 6:   463-468.

6. Kim JYH, Nelson AL, Algon SA, Graves O, Sturla LM, Goumnerova LC, Rowitch DH, Segal RA, Pomeroy SL: Medulloblastoma tumorigenesis diverges from cerebellar granule cell differentiation in patched heterozygous mice. Developmental Biology 263:50-66, 2003

7. Kitagawa H, Koie, Kanayama K, Sakail T. Medulloblastoma in a cat: clinical and MRI findings. *J Small Anim Pract.* 2003; 44: 139-142

8. Koestner A, Bilzer T, Schulman F, Summers B, Van Winkle T: Histological classification of tumors of the nervous system of domestic animals. *In: World Health Organization, International Histological Classification of Tumors of Domestic Animals, ed.* Armed Institute of Pathology, Washington, DC, 1999; 25-25

9. Krinke G, Kuafmann W, Mahrous A, Schaetti, P. Morphologic characterization of spontaneous nervous system tumors in mice and rats. *Toxicol Pathol.* 2000; 28: 178-192

10. Madrioli L, Biserni R, Panarese S, Morini M, Gandini G, Bettini G. Immunohistochemical profiling and telomerase activity of a canine medulloblastoma. *Vet Pathol.* 2011; 48: 814-816

11. Maxie M G, Youssef S: The nervous system. In: Jubb, Kennedy, and Palmer's Pathology of domestic animals. Vol. 1. 5th ed., Elsevier, Edinburg, 2007; 450-451

12. Steinberg H, Galbreath EJ. Cerebellar medulloblastoma with multiple differentiations in a dog. *Vet Pathol.* 2005; 35:543-546.

CASE IV. WSC 1920 Conf 19 Case 4 (JPC 4033564).

Signalment: 16-year-old, female spayed Maine coon cat (*Felis catus*)

History: The cat originally presented for an acute episode of collapse, left hemiparesis, and increased respiratory rate and respiratory effort. Neurological examination revealed anisocoria, a left head turn, and ambulatory left hemiparesis with proprioceptive deficits in the left fore and

Spinal cord, cat.   Four large red raised nodules are present on the ventral aspect of the spinal cord from C3-C5.   (Photo courtesy of: Animal Medical Center, 510 East 62nd St. New York, NY 10065, http://www.amcny.org/)

Spinal cord, cat.   Cross section of one of the nodules demonstrating its extension and compression of the ventral funiculi.   (Photo courtesy of: Animal Medical Center, 510 East 62nd St. New York, NY 10065, http://www.amcny.org/)

hind limbs. The neuroanatomical localization was multifocal with suspicion for C1-C5 myelopathy. Hematology and serum biochemistry profile were unremarkable, with the exception of a moderately elevated creatine kinase (1024 IU/L, RI: 64-440 IU/L). Thoracic radiographs revealed a patchy interstitial lung pattern presumed secondary to parenchymal disease. MR imaging of the brain and cervical spinal cord revealed an ill-defined hyperintensity in the left ventrolateral portion of the spinal cord at the cranial aspect of the C3. No intracranial abnormalities were detected, and an incidental unilateral otitis media was observed. Cisternal CSF analysis revealed moderately increased protein (184 mg/dL) and a moderately increased nucleated cell count with a mixed cell pleocytosis (150 nucleated cells/uL, 52% small mononuclear cells/mature lymphocytes, 27% nondegenerative neutrophils and 21% large monocytoid mononuclear cells with scattered erythrocytes and rare

erythrophagia). A vascular event was the most likely differential, but infectious etiologies could not be completely ruled-out. Titers for *Cryptococcus* and *Toxoplasma* were declined by the owner. The following day the cat's neurological examination and ability to ambulate had already improved. The cat was discharged with antibiotics and instructions to recheck with the neurology service and consult with the cardiology department. Serial neurological examinations revealed mild persistent paraparesis.

Eighteen months later the cat represented in congestive heart failure with a history of chronic progressive paraparesis. The owner elected euthanasia.
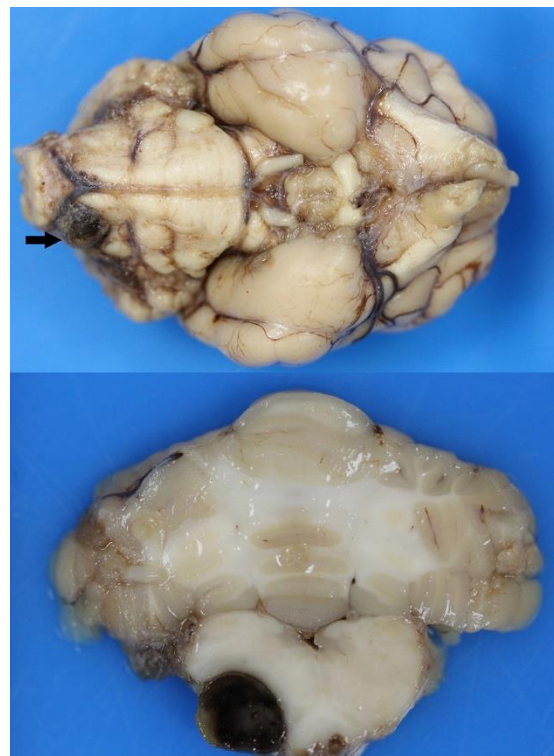

Spinal cord, cat.   A similar blood-filled nodule is present arising from the basilar artery at the ventral lateral aspect of the medulla.   (Photo courtesy of: Animal Medical Center, 510 East 62nd St. New York, NY 10065, http://www.amcny.org/)

Gross Pathology: Macroscopic examination of the spinal cord revealed four large, multifocal, dark red, raised nodules (presumed telangiectasia) at the ventral aspect of the mid body of C3-C4 and C4-C5, involving the cervical intumescence. These foci ranged from 3 x 2 mm to 1 mm in diameter. An additional, similar, small, dark red focus at ventral midline of the distal thoracic spinal cord measured approximately 1 mm in diameter, and three dark red, slightly raised, nodules were present on the ventral aspect of the lumbar spinal cord at L3 and L4, the largest measuring 5 x 2.5 mm (Figure 1B). When the nodules were sectioned, they were found to be homogenously dark red, and extended into the spinal cord parenchyma, at least 2.5 mm into the cervical segments (Figure 2), and 3 mm into the lumbar segments. In the brain, a large, well-demarcated, dark red, homogeneous, firm, round mass at the ventral lateral aspect of the medulla measured 6 x 5 x 7 mm and was adjacent to a branch of the basilar artery (arrow, Figure 3). When sectioned, the mass was well-demarcated, homogeneously dark red, and compressed the adjacent medullary parenchyma (Figure 3). A nodule in the left thyroid gland was observed, and the heart was moderately enlarged with dilation of the left atrium and auricle. There was no evidence of thromboembolism in the caudal aorta or iliac arteries.

Laboratory results: Serum biochemistry profile revealed a mildly elevated T4 concentration (5.0 ug/dL, (RI: 0.8-4.7 ug/dL) and mild azotemia (BUN 51 mg/dL, RI: 14-36 mg/dL; creatinine 2.0 mg/dL, RI: 0.6-2.4 mg/dL).

Microscopic Description:

Microscopic evaluation of the spinal cord revealed severe aneurysmal dilation of the ventral spinal artery at C3-4, C4-5 (Figure 4), L3 and L4. The tunica intima and media of the dilated vessels were thickened by deposition of hyaline, acellular eosinophilic material (hyalinosis, Figure 5) and occasionally, increased populations of spindle cells. In regions of most severe arterial dilation, the arterial wall was attenuated. Luminal thrombi were present within the affected arteries, with foci of re-canalization. Intramural arterial and periarterial hemorrhage was observed, with periarterial hemosiderin- and hematoidin-containing macrophages (Figure 6), sometimes intermixed with lymphocytes and plasma cells. These severely dilated vessels compressed the adjacent parenchyma. The ventral funiculi of the cervical and lumbar spinal cord exhibited variable amounts of white matter myelin vacuolation, with swollen, eosinophilic axons (spheroids), rare myelomacrophages, increased populations of glial cells, including microglia with rod morphology and reactive astrocytes, few Gitter cells, hemorrhage, and accumulation of eosinophilic material (possible edema). Within the ventral grey matter of the lumbar section, there was mild hemorrhage. Few corpora amylacea and Rosenthal fibers were present, most notably in the section of lumbar spinal cord. Occasional aggregates of eosinophilic material were observed in spinal nerves. A focus of hemorrhage intermixed with few hemosiderin containing macrophages was adhered to the dura in a section of cervical spinal cord. In regions of vascular hyalinosis, Congo Red stains were
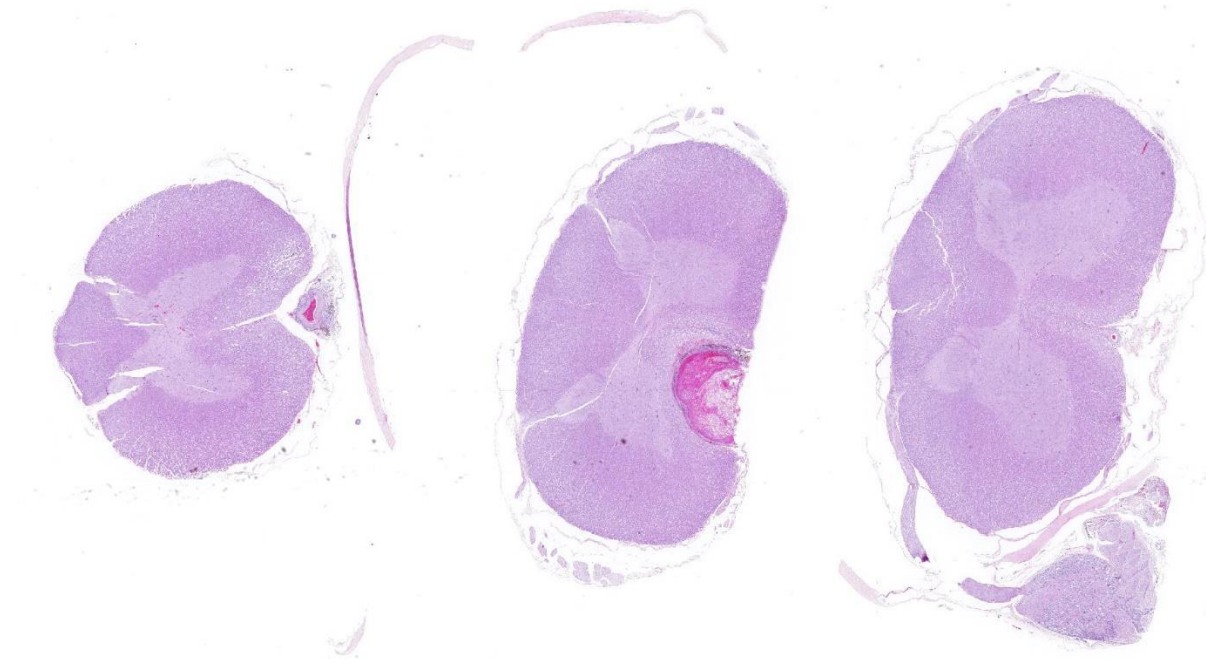
Spinal cord, cat. Three sections of cervical spinal cord are submitted, with thrombosis and marked dilation of the middle spinal artery present in the section in the middle. On the section at the left, the artery is patent, but the wall is markedly thickened. (HE, 8X)

negative for amyloid, and hyaline material stained magenta with Periodic acid Schiff (PAS) stains (Figure 7).

Histologic evaluation of the medullary mass in the brain (not included) revealed a severely dilated, thrombosed artery, adjacent to a lateral branch of the basilar artery (presumed to represent a communicating branch), with compression of the surrounding brain parenchyma and midline shift at the level of the olivary nucleus and deep arcuate fibers. Vessels were attenuated or the tunica intima and media were thickened by deposition of hyaline, acellular eosinophilic material (hyalinosis) and less frequently, spindle cell populations, with thrombosis, mural hemorrhage, periarteriolar hemosiderin-containing macrophages and lymphocytes. Congo red stains were negative for amyloid in regions

of arterial hyalinosis. The regional white matter exhibited myelin vacuolation, spheroid formation and necrosis, characterized by white matter rarefaction and Gitter cell infiltration, with rare neuronal chromatolysis and necrosis.

Contributor's Morphologic Diagnosis:

Spinal cord (cervical and lumbar segments): Severe, focal to multifocal ventral spinal hyaline arteriopathy (arteriolosclerosis) with severe dilation, thrombosis, intramural and periarteriolar hemorrhage and hemosiderosis

Spinal cord (cervical and lumbar segments): Severe, ventromedial white matter vacuolation with spheroid formation, gliosis, edema and hemorrhage

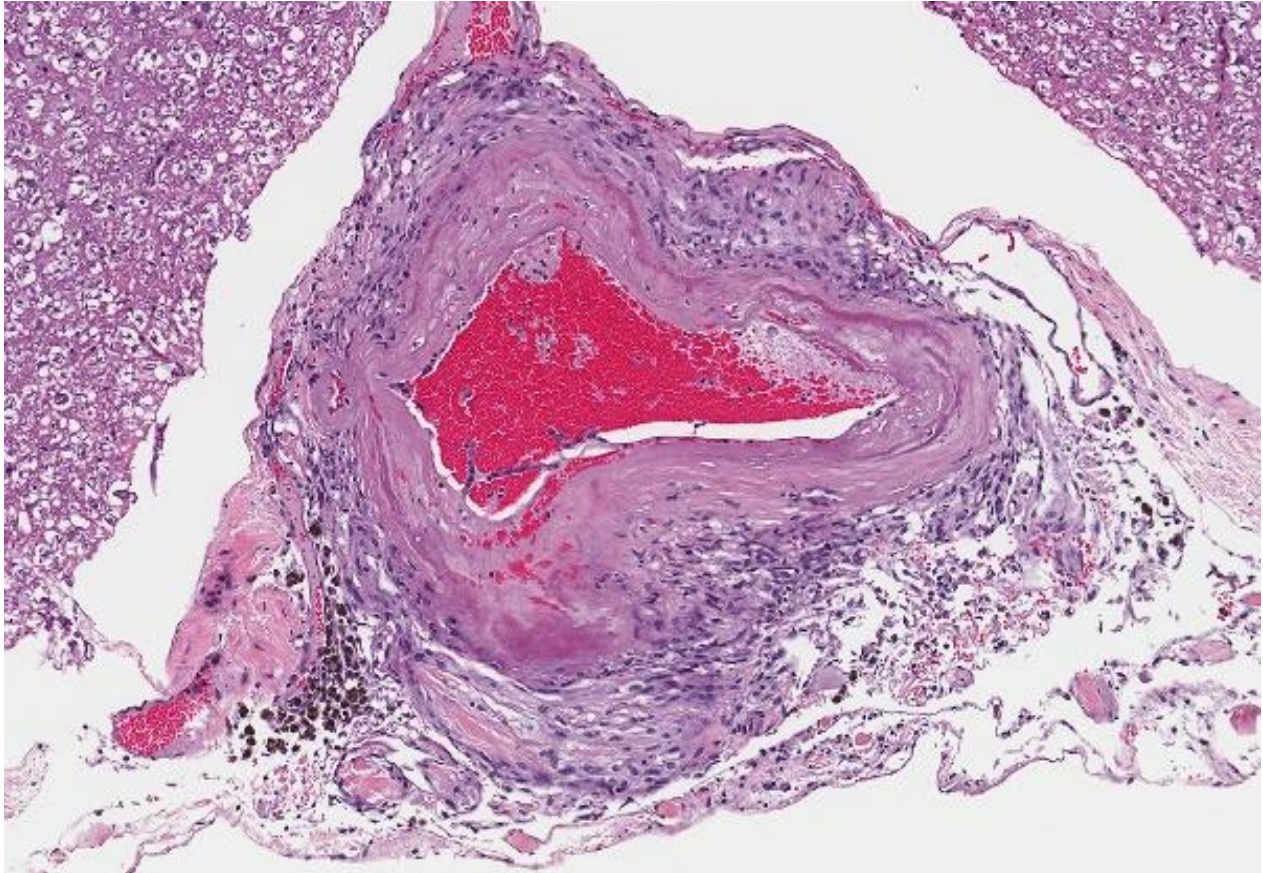**Contributor's Comment:** The ventral spinal artery was severely dilated,
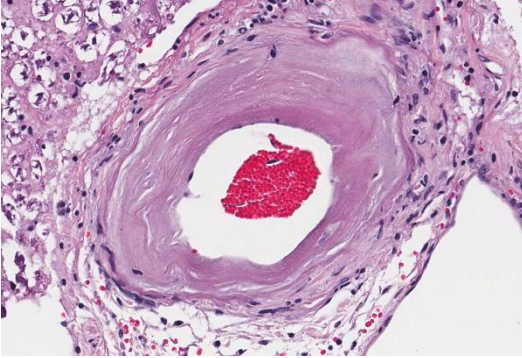
Spinal cord, cat. The tunica media of affected vessels contains a patchy deposition of hyaline eosinophilic protein, collagen and the adventitia contains circumferential lamellar collagen and fibrocytes. (HE, 100X) (Photo courtesy of: Animal Medical Center, 510 East 62nd St. New York, NY 10065, http://www.amcny.org/)

thrombosed, and thickened by deposition of hyaline material, resulting in grossly visible lesions. Damage to the spinal cord was interpreted to be multifactorial, caused by both ischemic and compressive damage. Arteriosclerosis literally translates to "hardening of the arteries" and in veterinary medicine, encompasses arteriolosclerosis and atherosclerosis. In humans, arteriosclerosis includes the two aforementioned categories as well as Monckeberg medial calcific sclerosis.[3] These lesions all result in stiffening and thickening of the arterial wall.[3]

Arteriolosclerosis is defined as a lesion of arterioles, which are small arterial vessels with 1 or 2 layers of smooth muscle cells.[3] Arteriolosclerosis includes hyaline and hyperplastic lesions.[1,,3,8] In humans, arteriolar hyalinosis occurs with benign hypertension and is associated with impaired autoregulation, hypothesized to be caused by hemodynamic injury with leakage of plasma components into the vessel wall.[1,9] This

lesion can also be seen with aging, diabetes mellitus, and focal segmental glomerulosclerosis (FSGS).[9] Hyperplastic arteriolosclerosis in people is more commonly linked to malignant hypertension, the histologic changes of which includes thickening of the arteriolar wall by concentric layers of hyperplastic smooth muscle cells. Recommendations have been made to term the hyaline subtype as intimal hyalinosis and hyperplastic arteriolosclerosis as fibromuscular intimal thickening.[3]

Hypertension has been linked to arteriolosclerosis in cats, reported in association with chronic renal disease, hyperthyroidism, primary hyperaldosteronism, and chronic anemia.[4,6,7] Between 65 and 100% of cats with systemic hypertension and concurrent hypertensive ocular lesions have evidence of reduced renal function.[4] However, this relationship is complex, and it cannot always be determined whether systemic hypertension is a cause or consequence of renal damage.[4] Systemic hypertension may be less prevalent in the hyperthyroid feline population than previously thought (reported ranges from 9-23%), and approximately 20% will develop hypertension following treatment, although not all will be azotemic.[4] Feline target organs that can incur damage secondary to hypertension include the eye, kidney, central nervous system and cardiovascular system.[4,6] The effects of hypertension on the eyes and heart have been described in cats.[4,6,7] Hypertensive encephalopathy in the

Spinal cord, cat. The tunica media of affected vessels contains a patchy deposition of hyaline eosinophilic protein, collagen and the adventitia contains circumferential lamellar collagen and fibrocytes. (HE, 100X) (Photo courtesy of: Animal Medical Center, 510 East 62nd St. New York, NY 10065, http://www.amcny.org/)

cat typically occurs following a precipitous and sustained rise in blood pressure that exceeds the limits of cerebral arterial autoregulation.[1]

Experimentally induced hypertensive encephalopathy in 2 cats was described.[1] Macroscopic abnormalities included cerebellar herniation, external hemorrhages and widening and flattening of the cerebral gyri (edema). Histologic evaluation revealed severe pallor and rarefaction of the cerebral white matter with regional widening of periarteriolar spaces and accumulation of PAS positive protein droplets. Vascular lesions were described as arteriolar

hyalinosis and hyperplastic arteriolosclerosis of pial arterioles. Rare ischemic changes and microhemorrhages were also found within the brain.[1] The pathogenesis is thought to involve autoregulatory failure of cerebral arterial blood flow during elevations of blood pressure. Forced vessel overdistension leads to blood brain barrier breakdown, opening of endothelial tight junctions and leakage of plasma proteins into the extracellular space and formation of vasogenic edema. Vascular dilation often starts segmentally, but can become diffuse, leading to generalized, interstitial cerebral edema. Clinical signs of hypertensive

encephalopathy in cats can include ataxia, lethargy, seizures, stupor, and blindness.[1]

In this case, hypertension was documented (200 mmHg), and the cat had a history of hyperthyroidism, mild azotemia, cardiomyopathy and moderate histologic lesions in the kidneys consistent with chronic renal disease. Based upon the ACVIM consensus guidelines for classification of blood pressure, this cat is in risk category IV, with severe risk of target organ damage.[4] Thus, hypertension may have played a role in the formation of hyaline arteriopathy, however, the reason for the predilection in the CNS for the ventral spinal artery, basilar artery and branches is unknown. It is possible that thrombosis may have played a role in the formation of these changes, although similar vascular lesions were observed in the lungs and heart. The diameter of the ventral spinal artery in cats is the smallest at the level of C2, which is a potential predisposing factor for thrombosis.[10] Evaluation of the brain did not reveal the histologic changes described in the experimentally induced hypertensive cats[1] and histologic retinal arteriolar changes were not identified. Aneurysmal dilation of the ventral spinal artery has not been previously described as a sequel to hypertension in cats, however, ischemic lesions in the spinal cord of cats have been frequently reported.[6,10,11] Predisposing medical conditions were reported to include chronic renal disease, hypertension, cardiomyopathy, and hyperthyroidism.[10,11] In one case series of 19 cats with ischemic myelopathy, the most commonly affected regions of spinal cord included the C1-C5 (30%) and C6-T2 (30%) regions of the
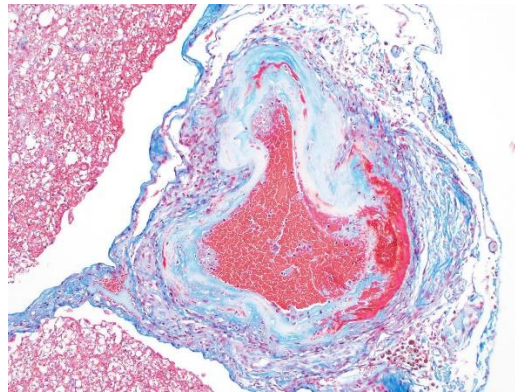
Spinal cord, cat. A Masson's trichrome stain highlights the deposition of collagen within the wall of damaged arteries. (Photo courtesy of: Animal Medical Center, 510 East 62nd St. New York, NY 10065, http://www.amcny.org/)

spinal cord, based upon MRI findings, with cervical spinal cord lesions in the region supplied by the ventral spinal artery.[11]

Although not present in this case, atherosclerosis is a lesion of arteriosclerosis in which fatty degenerative changes occur, and are typified by the presence of atheroma or fibrofatty plaque formation. In dogs, lipid is more frequently observed in the tunica media and adventitia, as opposed to the tunica intima in humans.[7] Atherosclerotic susceptibility amongst animals is variable, with atherosensitive species including humans, rabbits, chickens and pigs, and atheroresistant species including dogs, cats, cattle, goats and rats. In dogs, atherosclerosis is almost always found in conjunction with endocrine diseases, most notably hypothyroidism and diabetes mellitus.[7]

Contributing Institution:

Animal Medical Center, 510 East 62nd St. New York, NY 10065

http://www.amcny.org/
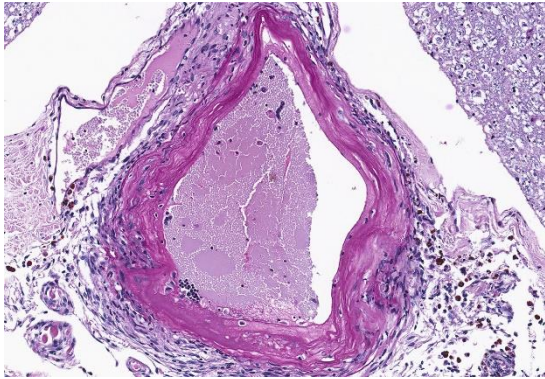
Spinal cord, cat. Hyaline material stains strongly positive with PAS. (Photo courtesy of: Animal Medical Center, 510 East 62nd St. New York, NY 10065, http://www.amcny.org/)

JPC Diagnosis: 1. Ventral spinal artery: Arteriosclerosis, diffuse, severe with aneurysmal dilatation, thrombosis, recanalization, and mural hyaline degeneration, and fibrosis.

2. Spinal cord, ventral funiculi: Axonal degeneration and loss, diffuse, mild to moderate.

JPC Comment: The contributor has provided an excellent review of hypertension and subsequent vascular change in cats. This particular case was subsequently published by Rylander et al.[10] in 2014, as part of a case series involving 5 cats.

Vascular disease resulting from feline hypertension has been previously seen in the Wednesday Slide Conference in 2017 (hypertensive retinopathy), and 2010 (hypertensive encephalopathy). While a common thread of chronic renal disease is associated with most cases[1] (and seen in this case), a number of other conditions may be responsible for hypertension in cats as well: hyperthyroidism (also noted in the clinical history in this case), diabetes mellitus, pheochromocytoma, hyperaldosteronism, and erythropoietin therapy.[5]

The pathogenesis of hypertensive encephalopathy is thought to involve the development of vasogenic edema as a result of sudden increases in blood pressure that exceed the autoregulatory capacity of the vasculature in the brain, resulting in endothelial injury and breakdown of the blood-brain barrier.[5] A recent publication by the moderator[2] has detailed the systemic pathology and resultant vascular and parenchymal lesions of feline hypertensive encephalopathy. In this case review of 12 cats, the median age was 12 years, without apparent breed predilection. All 12 had measured hypertension, from 16—300mm Hg. 11 of 12 animals had chronic tubulointerstitial nephritis and 4/12 had concurrent hyperthyroidism (which is consistent with previous publications). 6/12 had choroidal arteriopathy, and 5/12 had left ventricular hypertrophy.[2]

Neurological signs were most often localized to the prosencephalon and/or posterior fossa (brainstem and cerebellum), with 8/12 casts demonstrating cranial neve deficits, 50% had altered mentation ranging from dull to comatose. 5/12 developed seizure activity.[2]
]

Gross lesions were only seen in 4/12 cases, to include cerebral edema with or without displacement of the cerebellum. In this study, the primarily histologic lesion was bilaterally symmetrical regional to diffuse cerebral edema of the white matter, most severe at the dorsal aspect of white matter tracts.[2] Areas of edema separated myelin sheaths, and were populated by subjectively increased numbers of glial cells, including Alzheimer II astrocytes; gemistocytic astrocytes were seen in 3/12 cases.

Leptomeningeal arteriosclerosis was identified in 9/12 cases, with 8 of 12 demonstrating hyaline change. Lamellar fibrosis of the serosa ("onion-skinning") was relatively uncommon, being seen in 2 cases, one with the highest arterial pressure, and one with the longest history of systemic hypertension.[2]

References:

1. Brown CA, Munday JS, Mathur S, Brown SA. Hypertensive encephalopathy in cats with reduced renal function. *Vet Pathol*. 2005; 42:642-649.

2. Church ME, Turek BJ, Durham AC. Neuropathology of spontaneous hypertensive encephalopathy in cats. *Vet Pathol* 2019; 56(5):778-782.

3. Fishbein GA, Fishbein MC. Arteriosclerosis, rethinking the current classification. *Arch Pathol Lab Med.* 2009; 133:1309-1316.

4. Jepson R. Feline systemic hypertension, classification and pathogenesis. *J Fel Med Surg*. 2011; 13:25-34.

5. Kent M. The cat with neurological manifestations of systemic disease; key conditions impacting on the CNS. *Journal of Feline Med Surg.* 2009;11:395-407.

6. Littman MP. Spontaneous systemic hypertension in 24 cats. *J Vet Intern Med*. 1994; 8:79-86.

7. Maggio F, DeFrancesco TC, Atkins CE, Pizzirani S, Gilger BC, Davidson MG. Ocular lesions associated with systemic hypertension in cats: 69 cases (1985-1998). *J Am Vet Med Assoc.* 2000; 217(5):695-702.

8. Maxie MG, Robinson WF. Cardiovascular system. In: Jubb, Kennedy, and Palmer's Pathology of Domestic Animals, vol 3, 5th ed. New York, NY: Elsevier Limited; 2007:56-61.

9. Olsen JL. Hyaline arteriolosclerosis: new meaning for an old lesion. Editorial. *Kidney Intl.* 2003; 63:1162-1163.

10. Rylander H, Eminaga S, Palus V, Steinberg H, Caine A, Summers BA, Gehrke J, West C, Fox PR, Donovan TA, Cherubini GB. Feline ischemic myelopathy and encephalopathy secondary to hyaline arteriopathy in five cats. *J Feline Med Surg* 2014; 16(10):832-9.

11. Theobald A, Volk H, Dennis R, Berlato D, DeRisio L. Clinical outcome in 19 cats with clinical and magnetic resonance imaging diagnosis of ischaemic myelopathy (2000-2011). J Fel Med Surg. 2012; 15(2): 132-141.